Biogeosciences, 20, 3613–3624, 2023
https://doi.org/10.5194/bg-20-3613-2023

Biogeosciences Open Access EGU

Bacterioplankton dark CO_2 fixation in oligotrophic waters

Afrah Alothman[1], Daffne López-Sandoval[1,2], Carlos M. Duarte[1], and Susana Agustí[1]

[1]Red Sea Research Centre, Biological and Environmental Science and Engineering Division, King Abdullah University of Science and Technology (KAUST), Thuwal, 23955, Saudi Arabia
[2]Coastal and Marine Resources Core Lab (CMR), King Abdullah University of Science and Technology (KAUST), Thuwal, 23955, Saudi Arabia

Correspondence: Afrah Alothman (afrah.alothman@kaust.edu.sa)

Received: 9 April 2023 – Discussion started: 24 April 2023
Revised: 20 June 2023 – Accepted: 1 August 2023 – Published: 31 August 2023

Abstract. Dark CO_2 fixation by bacteria is believed to be particularly important in oligotrophic ecosystems. However, only a few studies have characterized the role of bacterial dissolved inorganic carbon (DIC) fixation in global carbon dynamics. Therefore, this study quantified the primary production (PP), total bacteria dark CO_2 fixation (TB_{DIC} fixation), and heterotrophic bacterial production (HBP) in the warm and oligotrophic Red Sea using stable-isotope labeling and cavity ring-down spectroscopy (^{13}C–CRDS). Additionally, we assessed the contribution of bacterial DIC fixation (TB_{DIC} %) relative to the total DIC fixation ($total_{DIC}$ fixation). Our study demonstrated that TB_{DIC} fixation increased the $total_{DIC}$ fixation from 2.03 to 60.45 $\mu g\,C\,L^{-1}\,d^{-1}$ within the photic zone, contributing 13.18 % to 71.68 % with an average value of 33.95 ± 0.02 % of the photic layer $total_{DIC}$ fixation. The highest TB_{DIC} fixation values were measured at the surface and deep (400 m) water with an average value of 5.23 ± 0.45 and $4.95 \pm 1.33\,\mu g\,C\,L^{-1}\,d^{-1}$, respectively. These findings suggest that the non-photosynthetic processes such as anaplerotic DIC reactions and chemoautotrophic CO_2 fixation extended to the entire oxygenated water column. On the other hand, the percent of TB_{DIC} contribution to $total_{DIC}$ fixation increased as primary production decreased ($R^2 = 0.45$, $p < 0.0001$), suggesting the relevance of increased dark DIC fixation when photosynthetic production was low or absent, as observed in other systems. Therefore, when estimating the total carbon dioxide production in the ocean, dark DIC fixation must also be accounted for as a crucial component of the carbon dioxide flux in addition to photosynthesis.

1 Introduction

Bacteria are the central nodes of the microbial loop and play an essential role in the flux of organic carbon in marine ecosystems through different metabolic pathways (Azam et al., 1983). Most studies on the metabolism of marine bacteria have focused on quantifying the uptake of organic compounds by heterotrophic bacteria and how it relates to bacterial growth and reproduction (Ducklow and Kirchman, 2000; Kirchman, 2000). However, heterotrophic marine bacteria can also metabolize CO_2 through anaplerotic carboxylation reactions, which form the basis of several metabolic pathways (Dijkhuizen and Harder, 1984). Such reactions are essential components of metabolic pathways in bacteria that enable the synthesis of fatty acids, amino acids, vitamins, and nucleotides (Dijkhuizen and Harder, 1984; Erb, 2011), which also fuel microbial food webs.

Wood and Werkman (1936) first proposed that heterotrophic bacteria contribute to dark dissolved inorganic carbon (DIC) fixation, a discovery that was widely embraced by the scientific community. A decade later, when radioactive isotope techniques emerged in the field, Steemann-Nielsen (1952) first reported on the possible importance of dark DIC fixation to the total carbon flux in the ocean, suggesting that it could represent between 1 % and 30 % of photosynthetic CO_2 fixation (Steemann-Nielsen, 1952; Nielsen, 1960). Subsequent quantifications in the northern to southern Pacific and Atlantic oceans reported that dark DIC fixation accounted for approximately > 10 % of photosynthetic CO_2 fixation in temperate and equatorial areas and between 10 % and 50 % of the light fixation rate in subtropical gyres (Prakash et al., 1991). Indeed, dark CO_2 assimilation con-

tributes considerably to DIC fixation in marine surface water, which has been directly associated with high bacterial activity and production (Prakash et al., 1991; Li et al., 1993; Markager, 1998; Li and Dickie, 1991; Alonso-Sáez et al., 2010). A study that evaluated the role of Arctic bacterial dark CO_2 incorporation suggested that the depletion and limitation of labile organic carbon compounds could enhance the utilization of bicarbonate by chemoautotroph or heterotroph microorganisms to achieve metabolic balance (Alonso-Sáez et al., 2010). In general, anaplerotic CO_2 fixed by some bacterial species has been reported to increase bacterial cell production by 1 %–6.5 % in incubated cultures (Roslev et al., 2004) and contributes significantly to the carbon flux dynamics of many marine ecosystems (Alonso-Sáez et al., 2010; Yakimov et al., 2014; Zhou et al., 2017; Signori et al., 2018; and Lliros et al., 2011).

Dark CO_2 fixation by marine bacteria is thought to play an essential role under oligotrophic conditions, contributing up to 30 % of bacterial production (González et al., 2008; Palovaara et al., 2014). A discovery of light-driven CO_2 incorporation by proteorhodopsin-containing flavobacterium *Polaribacter* sp. highlighted the significant role of anaplerotic metabolism in heterotroph life (González et al., 2008). Additionally, a genetic study conducted in the Atlantic Ocean has demonstrated that organic-matter-enriched samples showed an increase in the abundance of associated anaplerotic enzyme transcripts coincident with a sudden increase in bacterial abundance (Baltar et al., 2016). Therefore, whereas the total primary production of oceanic ecosystems is typically attributed to photosynthesis, dark chemoautotrophic and anaplerotic metabolism can also contribute 5 %–22 % to the total DIC fixation (Baltar and Herndl, 2019).

Dark CO_2 fixation by bacteria is, therefore, likely to be highly relevant in the Red Sea, a predominantly oligotrophic, landlocked system with no river inflow and with limited connection to the Indian Ocean (Edwards, 1987; Grasshoff, 1969). These features result in a limited nutrient input and an oligotrophication decreasing gradient from south to north (Wafar et al., 2016). The Red Sea is also characterized by high surface temperatures ranging from 20 to 33.1 °C (Chaidez et al., 2017; Shaltout, 2019) and warm deep-water temperatures of up to ∼ 21.5 °C at depths below 300 m (Yao and Hoteit, 2018).

In our study, we hypothesized that there is a substantial involvement of dark CO_2 fixation to the total DIC fixation within the Red Sea, increasing toward the most oligotrophic waters. Here we assess the contribution of dark CO_2 assimilation to the Red Sea bacterioplankton production using a ^{13}C stable isotope as a tracer. In this study, both the dark bicarbonate synthesis by bacteria (TB_{DIC}) and light bicarbonate synthesis by photosynthetic phytoplankton (PP) were quantified using ^{13}C as a tracer in the Red Sea water column. Additionally, ^{13}C stable-isotope fluxes were used to estimate bacterial production (BP) in the dark. Our study also assessed the variations in dark CO_2 fixation rates at different depths through the water column in both open and coastal water bodies and the relationship with water temperature. Moreover, our study estimated the contribution of dark bicarbonate synthesis (TB_{DIC} %) to total CO_2 fixation ($total_{DIC}$ fixation) by accounting for dark and light CO_2 fixation rates.

2 Methods

2.1 Sample collection and processing

A total of 59 water samples were collected over the course of four oceanographic cruises in the eastern Red Sea, including the Center Competitive Found (CCF), Deep Cruise (DC), Deep Coral Survey (DCS), and Red Sea Decade Expedition (RSDE). Samples were also obtained from a time series fixed station (pelagic) and two other coastal sites (a lagoon and reef located in Abu Shushah) in the central Red Sea of Saudi Arabia (Fig. 1). The cruises were conducted on board R/V *Thuwal* (DC, DCS), R/V *Al Azizi* (CCF), and R/V *OceanXplorer* (RSDE) between August 2017 and June 2022. Water samples during this study were collected from surface water ranging from 3–5 m (CCF, DC, DCS, RSDE, time series and coastal stations), adding four to five different photic layer depths in the water column, ranging from 12–90 m during the CCF cruise, and deep-water samples collected at 400 m during the RSDE cruises. Water samples were collected in the early morning using 12 L Niskin bottles with a rosette system (López-Sandoval et al., 2021) or 10 L Niskin bottles deployed manually for some surface water sampling. For the deep water (400 m), the water samples were collected using 1.5 L Niskin bottles attached to a remotely operated underwater vehicle (ROV) or in a submarine for RSDE on board R/V *OceanXplorer*. Data of seawater temperature, salinity, and underwater photosynthetic active radiation were obtained from CTD (conductivity, temperature, and depth electronic Sea-Bird SBE 911Plus) deployments for the studied coastal and open-water stations (Table 1) as described in López-Sandoval et al. (2021).

At each station, water samples for isotope labeling analyses were collected in the morning using 12 L Niskin bottles with a rosette system or 10 L Niskin bottles deployed manually (López-Sandoval et al., 2021). For the deepest water (400 m), the water samples were collected using 1.5 L Niskin bottles attached to a remotely operated underwater vehicle (ROV) and a submarine on board R/V *OceanXplorer*. Water samples were collected directly from the Niskin bottles, prefiltered through 100 µm mesh filters to remove larger zooplankton, and transferred into 10 L acid-washed carboy containers. The water samples were distributed into three transparent 2 L or 500 mL (^{13}C–PP; López-Sandoval et al., 2019) polycarbonate (PC) bottles for light primary production measurements and another three dark 2 L or 500 mL PC bottles for measuring dark bacterial DIC uptake rate (^{13}C–TB_{DIC}). All water samples were enriched with sodium

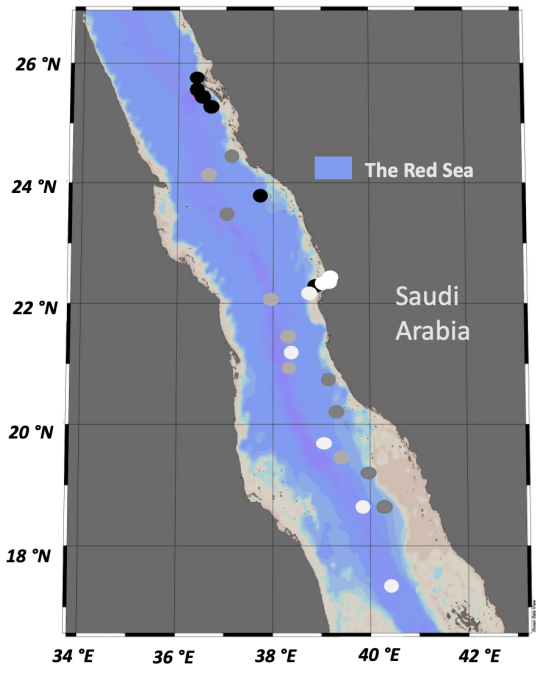

Figure 1. Stations sampled during the four oceanographic cruises – DCS (black dots), DC (dark-gray dots), RSDE (light-gray dots), CCF, time series and coastal stations (white dots) – along the eastern Red Sea conducted between 2017 and 2022.

bicarbonate-^{13}C solution (99.8 at. % 4 g L^{-1} of $NaH^{13}CO_3^-$; López-Sandoval et al., 2019) to a final carbon concentration of ∼ 153 µmol $^{13}C\,L^{-1}$ in each bottle. Additionally, during the DC and DCS oceanographic cruises, three dark PC bottles were enriched with D-glucose-$^{13}C_6$ substrate at a final concentration of 100 nM to measure bacterial production (^{13}C–BP) as described by Koshikawa et al. (1999). All PC bottles were incubated in tanks placed on the vessel's deck with a circulating seawater system to maintain surface water temperature and receive natural solar radiation. Moreover, a separate tank was attached to a chiller to mimic the water temperature at a 400 m depth. Additionally, coastal water samples were incubated in a similar outdoor setup at the Coastal & Marine Resources Core Lab (CMR) at King Abdullah University of Science and Technology (KAUST).

The bottles for PP were covered with neutral-density nets to reduce the light intensity according to the matching light received at the assigned depth in concordance with CTD profiles. After 4–6 h of incubation, dark and light bottles samples from CCF cruise were filtered through pre-combusted Whatman GF/F filters (López-Sandoval et al., 2021). Incubated samples from other cruises were first filtered through 25 mm diameter 3 µm silver membranes (Sterlitech) followed by a filtration through 0.2 µm pore size silver membrane filters (25 mm diameter, Sterlitech). The collected filters were placed in small Petri dishes containing 150 µL (50 %) HCl to remove carbonate from the filters, allowed to dry for 12 h, and stored at −20 °C until required for downstream analyses. Moreover, the natural isotopic composition of particulate organic carbon was measured in the surface and deep seawater at each station in similar filters as indicated above (Whatman GF/F filters in CCF cruise and 0.2 µm pore size silver membrane the rest of cruises).

2.1.1 Chlorophyll-*a* concentration and nutrients

Samples for chlorophyll *a* (Chl *a*) and nutrient analyses were collected at each depth within the photic layer during the CCF cruise and from surface water during the time series (López-Sandoval et al., 2021) and DC, DCS, RSDE, and the coastal stations. Water samples (200–500 mL) were filtered through 25 mm Whatman GF/F filters (0.7 µm) and then extracted in 90 % acetone in the dark as described by Prabowo and Agusti (2019) and López-Sandoval et al. (2021). After 24 h, the extracted pigments were measured using a Trilogy Fluorometer equipped with a CHL–NA module (Turner Designs; San Jose, USA) calibrated with pure Chl *a* (Prabowo and Agusti, 2019). Water samples for inorganic nutrient concentration were collected and frozen until analyzed in the laboratory. Nutrient concentrations were determined with a Segmented Flow Analyzer (SEAL Autoanalyzer (AA) HR 3, Analytical Inc.; WI, USA) following standard autoanalyzer methods (Hansen and Koroleff, 1999).

2.1.2 Heterotrophic bacteria abundance

The abundance of heterotrophic bacteria was quantified in each water sample. Briefly, 1.8 mL aliquots were obtained from each sample, fixed with 25 % glutaraldehyde, flash-frozen in liquid nitrogen, and stored at −80 °C for later analysis. The samples were stained with SYBR Green I intermediate solution (1 : 100) for the determination of bacteria cell abundance by flow cytometry (Gasol and Morán, 2016) using either a FACSCanto II (Becton Dickinson) or a CyFlow Cube 8 (Sysmex).

2.1.3 Dissolved inorganic carbon (DIC)

The δ^{13}C of DIC in natural waters and after enrichment with $NaH^{13}CO_3^-$ was analyzed in seawater samples placed in 15 mL small glass tubes and treated with 0.05 % mercuric chloride ($HgCl_2$, Sigma-Aldrich) to stop any biological activity after sampling (Dickson et al., 2007). After fixation, all samples were kept in a dark and cool place until analysis in the laboratory. DIC measurements were conducted using an AutoMate Prep Device coupled with Picarro's Liaison interface and IsoCO_2 wavelength scan cavity-ring down spectroscopy (WS-CRDS) system (Santa Clara, California, USA).

2.1.4 Primary production (PP) and total dark bacteria DIC fixation (TB_{DIC})

The carbon content and the $\delta^{13}C$ values from PP and TB_{DIC} incubation filters were analyzed using a combustion module (CM) attached to a cavity ring-down spectroscopy analyzer (CM-CRDS-G2201-I, Picarro), and each filter was analyzed for 600 s. The combustion module converted the sample into the required gas (CO_2) by fast combustion, after which the gas was transferred to the isotopic analyzer to measure the $^{13}C/^{12}C$ ratio ($\delta^{13}C$). Inside the cavity, spectrum peaks were generated according to the measured wavelength absorbed by the gas of interest ($^{13}CO_2$ and $^{12}CO_2$), where each peak corresponded to the ^{13}C and ^{12}C concentrations (López-Sandoval et al., 2019).

Before analyzing the filters, a Picarro CRDS was calibrated using Vienna Pee Dee Belemnite (VPDB) standards from the International Atomic Energy Agency (IAEA) including IAEA-CH-6, C3, and 303B with $\delta^{13}C$ values of $-10.45\,‰$, $-24.72\,‰$, and $+450\,‰$, respectively. Additionally, Reston Stable Isotopic Laboratory standards (United States Geological Survey, UGS) were also used, including USG62 ($-14.79\,‰$), USG40 ($-26\,‰$, $39\,‰$), and USG41a ($+36.55\,‰$, López-Sandoval et al., 2019).

The ^{13}C and ^{12}C isotopic mass from the ^{13}C-enriched sample at the end of incubation time (h) was determined to calculate PP ($\mu g\,C^{-1}\,h^{-1}$) using the ^{13}C–CRDS–PP method (López-Sandoval et al., 2019). Particularly, ^{13}C–PP was calculated as the isotopic shift of particulate organic carbon (POC) from the samples incubated in the light ($\delta^{13}C_{POC_{Light}}$) relative to the dark isotopic composition of the samples ($\delta^{13}C_{POC_{Dark}}$). Additionally, the isotopic shift of the enriched DIC ($\delta^{13}C_{DIC_{Enriched}}$) relative to the natural DIC samples ($\delta 13C_{DIC_{Natural}}$) was also calculated. The production was converted to carbon uptake rates considering the particulate organic carbon measured at the end of incubation in the light-enriched samples per volume (v) filtered in liters (POC-$\mu g\,C\,L^{-1}$), and the carbon fixation rate was calculated per time unit (hours of incubation) following Eq. (1):

$$^{13}C\text{–}PP = \left(\left[\left(\delta^{13}C_{POC_{Light}} - \delta^{13}C_{POC_{Dark}}\right)\Big/ \left(\delta^{13}C_{DIC_{Enriched}} - \delta^{13}C_{DIC_{Natural}}\right)\right] \times POC/v/t\right). \quad (1)$$

The TB_{DIC} fixation rate ($\mu g\,C^{-1}\,h^{-1}$) was measured using a similar equation as for the ^{13}C–PP method. However, the uptake rate was calculated as the isotopic shift of particulate organic carbon from the samples incubated in the dark ($\delta^{13}C_{POC_{Dark}}$) relative to the natural isotopic composition of the samples ($\delta^{13}C_{POC_{Natural}}$). Additionally, we also calculated the isotopic shift of the enriched DIC ($\delta^{13}C_{DIC_{Enriched}}$) relative to the natural DIC samples ($\delta^{13}C_{DIC_{Natural}}$). The production rate was also converted to carbon uptake rates considering the particulate organic carbon measured at the end of incubation in the dark-enriched samples and the volume filtered in liters (POC-$\mu g\,C\,L^{-1}$). Additionally, the carbon fixation rate was calculated per time unit (hours of incubation) following Eq. (2):

$$^{13}C\text{–}TB_{DIC} = \left(\left[\left(\delta^{13}C_{POC_{Dark}} - \delta^{13}C_{POC_{Natural}}\right)\Big/ \left(\delta^{13}C_{DIC_{Enriched}} - \delta^{13}C_{DIC_{Natural}}\right)\right] \times POC/v/t\right). \quad (2)$$

The $total_{DIC}$ fixation was calculated as the sum of the ^{13}C–PP measured in the light and ^{13}C–TB_{DIC} measured in the dark following Eq. (3):

$$total_{DIC}\ \text{fixation} = {}^{13}C\text{–}PP_{Light} + {}^{13}C\text{–}TB_{DIC_{Dark}}. \quad (3)$$

The contribution of the TB_{DIC} to the total carbon production was calculated relative to the $total_{DIC}$ fixation following Eq. (4):

$$TB_{DIC}\% = \left({}^{13}C\text{–}TB_{DIC_{Dark}}\right)\Big/\left(total_{DIC}\ \text{fixation}\right) \times 100. \quad (4)$$

The data for PP and TB_{DIC} were converted to carbon uptake per day using a local photoperiod of 12 h of daytime for photosynthesis and 12 h of nighttime for dark DIC fixation.

2.1.5 Bacterial production (BP)

Bacterial production (BP) was measured based on glucose uptake (expressed in $\mu g\,C\,L^{-1}\,h^{-1}$) as described by Middelburg et al. (2000). ^{13}C incorporation was calculated as glucose uptake and defined as the difference between the fraction of ^{13}C in the natural isotopic composition sample ($F_{Natural}$) relative to the ^{13}C fraction in the enriched sample ($F_{Enriched}$) following Eq. (5):

$$\text{Glucose uptake rate (BP-}\mu g\,C\,L^{-1}\,h^{-1}) = \left(\left(F_{Enriched} - F_{Natural}\right) \times POC\right)\Big/\left(v/t\right), \quad (5)$$

where $F = {}^{13}C/({}^{13}C + {}^{12}C)$, which is also expressed as $R/(R+1)$, where R is the carbon isotope ratio obtained from the measured $\delta^{13}C$ values, and it is calculated following Eq. (6) (Middelburg et al., 2000):

$$R = \left(\delta^{13}C/1000 + 1\right) \times VPDB(\text{Vienna Pee Dee Belemnite}), \quad (6)$$

where VPDB = 0.0112372. Additionally, the uptake rate was calculated by considering the particulate organic carbon measured in the samples at the end of incubation per time unit (hours of incubation) and per volume filtered in liters. The BP rates were reported on a per-day basis considering a 24 h cycle.

2.1.6 Statistical analyses

All statistical analyses were conducted using the JMP PRO 16 software (JMP®, Version ⟨16.0.0⟩ SAS Institute Inc., Cary, NC, 1989–2019). A p value ≤ 0.05 was considered statistically significant. The relationship and correlation between variables were explored using Spearman's nonparametric correlations and linear regression, and means were compared using one-way ANOVA and Student's t test.

3 Results

The seawater temperature during the study period ranged from a minimum of 21.0 °C in deep waters (400 m depth) to a maximum of 32.2 °C in surface waters. As data were collected during different seasons; therefore, surface temperature did not show a clear latitudinal pattern. Salinity, on the other hand, ranged from 38.21 to 40.80 (Table 1) and increased significantly with latitude ($\rho = 0.71$, $p < 0.0001$). Our results indicated that silicate (SiO_2) levels were generally low, ranging from 0.44 to 1.65 µM, whereas phosphate (PO_4) ranged from undetectable to 0.31 µM. Both SiO_2 and PO_4 decreased with increasing latitude ($\rho = -0.42$, $p < 0.0007$, and $\rho = -0.51$, $p < 0.0001$, respectively). Nitrate (NO_3) (Table 1), however, did not exhibit any significant spatial variability throughout the study, with an average (± SE) low value of 0.57 ± 0.05 µM (mean ± SE) from the surface to a 30 m depth, and a higher mean value of 2.44 ± 0.55 µM below 30 m depth. Surface phytoplankton Chl-*a* concentration averaged 0.22 ± 0.05 and $0.34 \pm 0.09\,\mu g\,L^{-1}$ in the south and north stations, respectively. Coastal stations showed a close average Chl-*a* value of $0.38 \pm 0.05\,\mu g\,L^{-1}$, although they exhibited the highest individual values (Table 1). However, during winter in the northern stations, Chl-*a* concentration peaked and reached up to $0.69\,\mu g\,L^{-1}$, probably reflecting nutrient entrainment due to convective mixing. In addition, Chl-*a* concentrations measured during the CCF cruise through different photic zone layers showed an increase toward the maximum chlorophyll-*a* depth, located at 60–90 m depth, where it reached up to $0.48 \pm 0.036\,\mu g\,L^{-1}$.

Heterotrophic bacteria cell abundance ranged from 1.90×10^4 cells mL^{-1} at 400 m depth to 7.84×10^5 cells mL^{-1} in surface waters, averaging $3.78 \pm 0.38 \times 10^5$ cells mL^{-1} in the photic layer (Table 1). There was no significant difference in bacterial abundance between open and coastal water (F ratio = 0.19, degrees of freedom (df) = 1, $p = 0.66$). The bacterial production measured as the glucose uptake rate in the dark (HBP) varied from $0.04\,\mu g\,C\,L^{-1}\,d^{-1}$ recorded in the northern stations to 0.69 and $0.92\,\mu g\,C\,L^{-1}\,d^{-1}$ (Table 1) in the coastal reef and lagoon stations, respectively. Additionally, HBP was significantly different between coastal and open waters (F ratio = 11.07, df = 1, $p < 0.005$), with higher rates observed in the coastal stations ($0.60 \pm 0.21\,\mu g\,C\,L^{-1}\,d^{-1}$) compared to the open waters ($0.17 \pm 0.04\,\mu g\,C\,L^{-1}\,d^{-1}$). HBP increased with increasing temperature ($R^2 = 0.71$, $p < 0.0001$).

Primary production rates across the study ranged from 0.84 to $47.76\,\mu g\,C\,L^{-1}\,d^{-1}$ (Table 2) and were significantly higher at the coastal stations ($17.77 \pm 3.60\,\mu g\,C\,L^{-1}\,d^{-1}$) compared to open waters ($7.24 \pm 0.71\,\mu g\,C\,L^{-1}\,d^{-1}$) ($F$ ratio = 20.17, df = 1, $p < 0.0001$; Fig. 2a). PP also tended to increase with increasing temperature ($\rho = 0.35$, $p < 0.001$), but it was independent of Chl-*a* concentration ($\rho = 0.12$, $p = 0.52$) and declined with increasing nitrate concentration ($\rho = -0.46$, $p < 0.014$; Fig. 4). Primary production throughout the photic zone (CCF open water; Table 2) decreased from maximum $15.36\,\mu g\,C\,L^{-1}\,d^{-1}$ at the surface to $< 1\,\mu g\,C\,L^{-1}\,h^{-1}$ at the base of the photic layer (1 % PAR). Similarly, the concentration of particulate organic carbon across the photic layer changed gradually, from $95.13 \pm 10.23\,\mu g\,C\,L^{-1}$ at the surface to $18.25 \pm 1.28\,\mu g\,C\,L^{-1}$ at the base of the photic zone.

The ^{13}C dark TB_{DIC} fixation rate varied from $1.07\,\mu g\,C\,L^{-1}\,d^{-1}$ to a maximum of $12.69\,\mu g\,C\,L^{-1}\,d^{-1}$ (Table 2) with no latitudinal pattern. We found significant differences in TB_{DIC} between coastal ($6.92 \pm 0.81\,\mu g\,C\,L^{-1}\,d^{-1}$) and open-water stations ($3.34 \pm 0.37\,\mu g\,C\,L^{-1}\,d^{-1}$) ($F$ ratio = 19.89, df = 1, $p < 0.0001$; Fig. 2b) but not ($p = 0.84$) between surface ($5.24 \pm 0.54\,\mu g\,C\,L^{-1}\,d^{-1}$) and 400 m samples ($4.95 \pm 1.20\,\mu g\,C\,L^{-1}\,d^{-1}$), which showed the highest values compared to other depths (Fig. 3). Additionally, TB_{DIC} exhibited a weak relationship with HBP and bacterial abundance (Fig. 4), and, on average, TB_{DIC} ($4.09 \pm 0.38\,\mu g\,C\,L^{-1}\,d^{-1}$) exceeded the HBP rate ($0.26 \pm 0.06\,\mu g\,C\,L^{-1}\,d^{-1}$) by over 1 order of magnitude. We found no significant correlation between TB_{DIC} and temperature or nutrient concentration (Fig. 4). However, TB_{DIC} showed a high significant correlation with POC ($\rho = 0.80$, $p < 0.0001$) and a weak tendency to increase with increasing Chl *a* ($\rho = 0.38$, $p < 0.01$; Fig. 4).

The $total_{DIC}$ fixation rate, which is the uptake rate of both TB_{DIC} and PP fixation rates measured independently, ranged from 2.03 up to $60.45\,\mu g\,C\,L^{-1}\,d^{-1}$. We found a significant and positive correlation between TB_{DIC} fixation and PP ($\rho = 0.53$, $p < 0.0001$; Fig. 4). On average, the contribution of TB_{DIC} % to the $total_{DIC}$ daily fixation was 33.95 ± 0.02 %, ranging from 13 % to 72 % across samples (Table 2). The TB_{DIC} % contribution was independent of the absolute TB_{DIC} fixation rate ($R^2 = 0.05$, $p = 0.09$), and it was negatively correlated with PP ($R^2 = 0.45$, $p < 0.0001$; Fig. 5a) and did not differ between open and coastal waters (F ratio = 0.008, df = 1, $p = 0.92$). The high TB_{DIC} at 400 m (1.37 to $6.33\,\mu g\,C\,L^{-1}\,d^{-1}$; Table 2) implied that the contribution of TB_{DIC} at 400 m was high (40 %) relative to surface PP (Fig. 5b and Table 2).

4 Discussion

Although the contribution of heterotrophic bacteria to dark CO_2 fixation was discovered more than 80 years ago (Wood and Werkman, 1936), the number of studies quantifying dark heterotrophic bacteria CO_2 fixation are scarce (Braun et al., 2021), particularly relative to primary production rates. Our study successfully used the light and dark ^{13}C bicarbonate additions coupled with a Picarro CRDS to accurately quantify DIC incorporation by phytoplankton, heterotrophic bacteria, and chemoautotrophs during daytime and nighttime, respectively. Decades after Steemann Nielsen (1952) introduced the ^{14}C method to measure phytoplankton primary

Table 1. Value ranges (minimum–maximum) of the environmental and biological parameters obtained during the study along the Red Sea at different depths. The data in the table are chlorophyll-*a* concentration (Chl *a*), seawater temperature (Temp), salinity (Sal), nutrient concentrations (SiO_2, PO_4, and NO_3), heterotrophic bacteria abundance (BACT), and bacterial production (BP). NA: data not available.

Cruise	Date	Lat (° N)	Long (° E)	Depth (m)	Temp (°C)	Sal	Chl *a* ($\mu g\,L^{-1}$)	SiO_2 (μM)	PO_4 (μM)	NO_3 (μM)	BACT (cells mL^{-1})	BP ($\mu g\,C\,L^{-1}\,d^{-1}$)
CCF (open water)	16–21 Mar 2018	17.35–22.23	38.38–40.42	5–90	24.20–27.69	38.21–38.90	0.08–0.69	0.57–1.65	0.04–0.28	0.01–5.31	NA	NA
Deep Cruise (open water)	4–9 Apr 2019	18.67–24.46	37.01–40.22	5	24.00–27.00	38.30–40.00	0.14–0.19	0.59–1.03	0.06–0.20	0.14–0.60	3.25×10^5–7.84×10^5	0.12–0.46
Deep Coral Survey (open water)	18–23 Jan 2020	22.30–25.75	36.34–38.86	5	23.11–24.90	39.62–40.23	0.37–0.62	0.83–1.03	0.01–0.11	0.27–1.04	4.38×10^5–6.57×10^5	0.04–0.08
Time series (coastal)	21 Aug 2017–5 Feb 2018	22.31	38.96	3	24.40–32.10	39.30–39.57	0.18–0.81	0.44–1.02	0.01–0.31	0.44–1.12	2.00×10^5–4.13×10^5	NA
Reef (coastal)	12 Nov 2019	22.32	39.02	3	29.90	39.78	0.40	NA	NA	NA	NA	0.69
Lagoon (coastal)	22 Oct 2019	22.39	39.14	3	32.20	40.80	0.70	NA	NA	NA	NA	0.92
RSDE (open water)	7 Feb–5 Jun 2022	19.44–24.15	36.59–39.44	5	25.13–28.87	38.45–40.16	0.07–0.49	NA	NA	NA	5.87×10^4–1.86×10^5	NA
				400	21.00–21.72	39.29–40.54	NA	NA	NA	NA	1.90×10^4–3.48×10^4	NA

Table 2. Range (minimum–maximum) of dark DIC uptake rates by bacteria (TB_{DIC}), primary production (PP), the percentage contribution of TB_{DIC} (TB_{DIC} %) relative to the total DIC fixation ($total_{DIC}$ fixation), and PP obtained at different water depths in different cruises.

Cruise	Lat (° N)	Long (° E)	Depth (m)	TB_{DIC} ($\mu g\,C\,L^{-1}\,d^{-1}$)	PP ($\mu g\,C\,L^{-1}\,d^{-1}$)	PP %	TB_{DIC} %
CCF (open water)	17.35–22.23	38.38–40.42	5–90	1.07–2.69	0.84–15.36	28.22 %–86.82 %	13.18 %–71.78 %
Deep Cruise (open water)	18.67–24.46	37.01–40.22	5	2.05–12.45	2.69–16.71	45.48 %–70.87 %	29.13 %–54.52 %
Deep Coral Survey (open water)	22.30–25.75	36.34–38.86	5	2.69–10.61	3.16–14.68	34.49 %–82.68 %	17.32 %–65.51 %
Time series (coastal)	22.31	38.96	3	3.44–12.69	3.46–47.76	34.49 %–84.37 %	15.63 %–65.51 %
Reef (coastal)	22.32	39.02	3	3.44	4.31	55.61 %	44.39 %
Lagoon (coastal)	22.39	39.14	3	10.11	15.88	61.10 %	38.90 %
RSDE (open water)	19.44–24.15	36.59–39.44	5	1.89–5.65	2.15–6.21	48.13 %–75.55 %	24.45 %–55.43 %
RSDE (open water)	19.44–24.15	36.59–39.44	400	1.37–6.33	NA	NA	NA

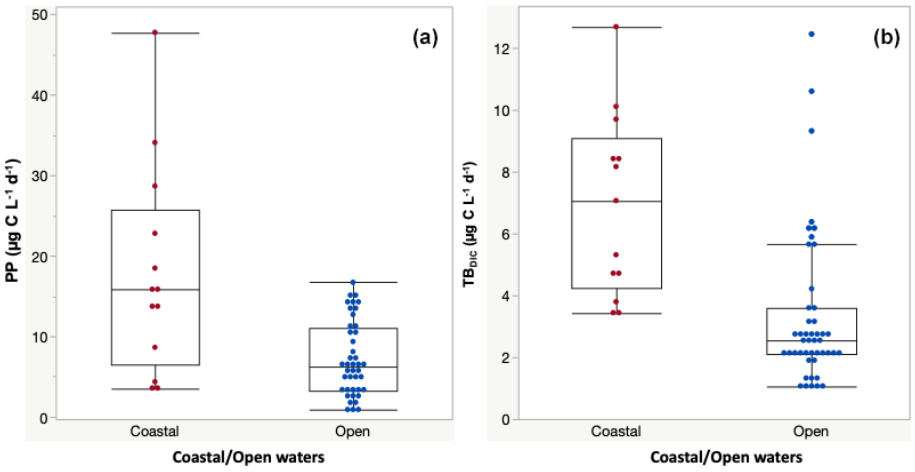

Figure 2. **(a)** Primary production (PP) and **(b)** total dark bacteria DIC fixation (TB_{DIC}) measured in coastal and open waters. Box plots indicate the 95 % confidence intervals with ± 1 SD. The central line in the box represents the median for each group of samples.

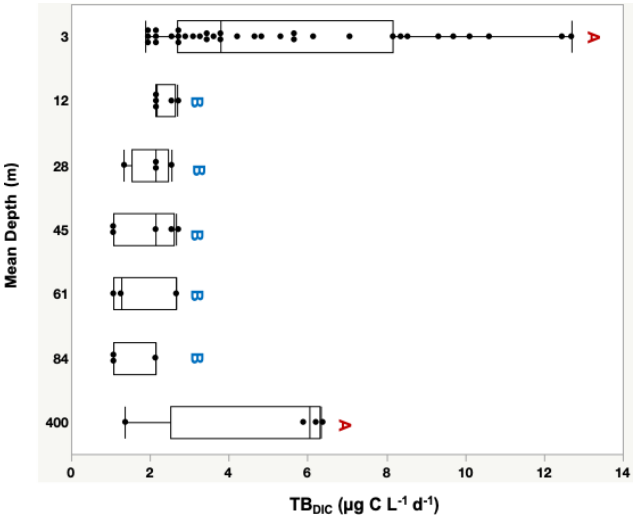

Figure 3. Total bacteria DIC uptake rate (TB_{DIC} µg C L^{-1} d^{-1}) measured at the photic zone (3–90 m), and in deep waters (400 m), where different letters indicate statistically significant differences ("A" is significantly higher than "B"). Each box plot indicates the 95 % confidence intervals with ± 1 SD. The central line in the box represents the median for each group of samples.

production, the ^{13}C–PP method has recently garnered increasing attention as an alternative to the use of radioactive isotopes. Here, we extend the use of ^{13}C bicarbonate additions to also resolve dark DIC uptake by bacteria, providing, to the best of our knowledge, the first application of this method coupled with a Picarro CRDS. Indeed, most previous studies measured dark DIC fixation using the ^{14}C bicarbonate method (Baltar et al., 2010; Reinthaler et al., 2010; Alonso-Sáez et al., 2010; Llirós et al., 2011; Yakimov et al., 2014; Zhou et al., 2017; Signori et al., 2018) or genome and 16S ribosomal analysis (González et al., 2008; Yakimov et al., 2014), whereas very few studies have used ^{13}C bicarbonate to measure dark DIC fixation (Roslev et al., 2004). One of the main advantages of using the stable isotope instead of radioactive isotopes addition is that it greatly reduces the health and safety issues associated with using radioactive products. Additionally, this method can be easily applied to characterize field samples (Middelburg et al., 2000; Boschker and Middelburg, 2002). Recent studies have demonstrated that the phytoplankton photosynthesis quantification results obtained with the ^{13}C–PP method coupled with a Picarro CRDS were similar to those achieved with the ^{14}C method (López-Sandoval et al., 2018, 2019). Cavity ring-down spectroscopy (CRDS), particularly with the Picarro analyzer, offers several advantages for stable-isotope analyses applications. CRDS can detect trace amounts of isotopes in samples with very high sensitivity. This makes it particularly useful for analyzing low-concentration samples like oligotrophic waters. The high sensitivity of CRDS also allows for high precision and accuracy in isotopic measurements (Berden et al., 2000; López-Sandoval et al., 2019).

Previous studies have confirmed that bacterial dark CO_2 uptake contributes significantly to the carbon flux dynamics of oligotrophic waters, shallow waters, coastal waters, and deep seas (Alonso-Sáez et al., 2010; Yakimov et al., 2014; Zhou et al., 2017; Signori et al., 2018; Llirós et al., 2011). Here, we independently calculated dark DIC uptake and PP, and we confirmed the relevance of the dark CO_2 fixation processes in the oligotrophic Red Sea. Our estimates were within the range of reported dark DIC fixation rate, which ranges from 0.001 µg C L^{-1} d^{-1} in surface waters of the subtropical North Atlantic and tropical estuarine systems (Reinthaler et al., 2010; Signori et al., 2018) to 206 µg C L^{-1} d^{-1} in an eutrophic Mediterranean lagoon (Llirós et al., 2011). In contrast, the highest values recorded in our study were found in coastal waters and were similar

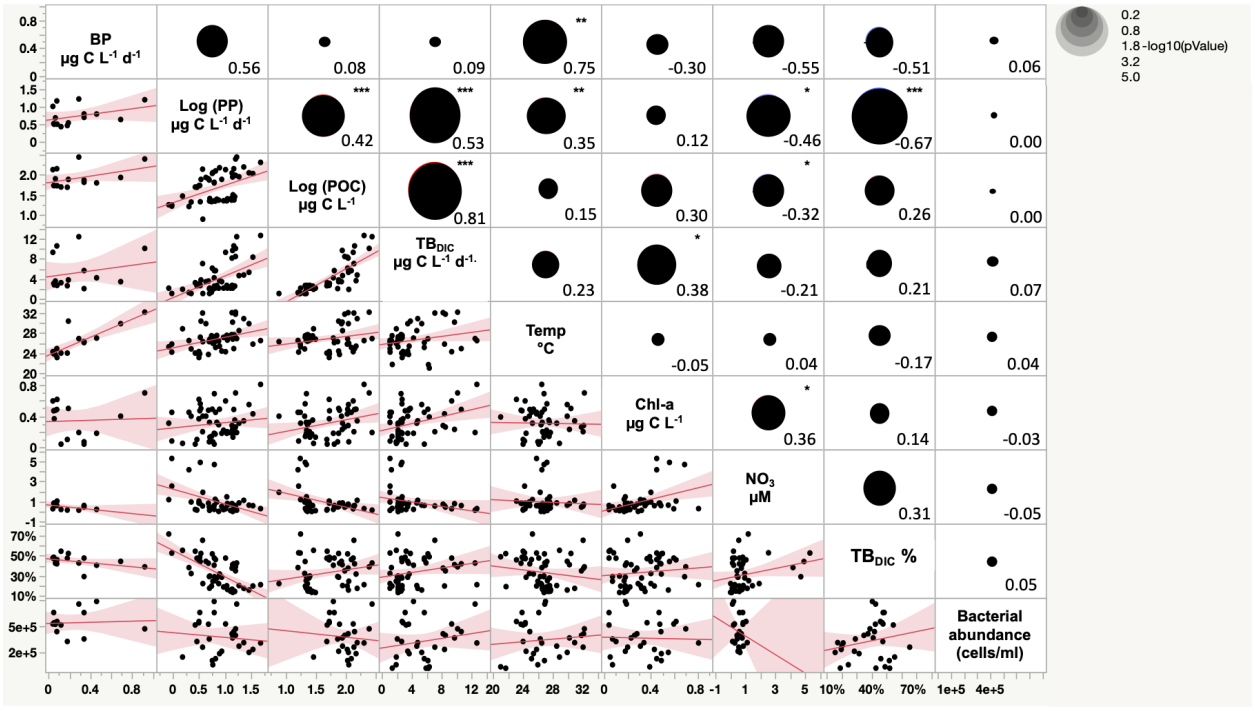

Figure 4. Scatterplot matrix plot (lower diagonal) and Spearman correlation coefficient (upper diagonal) among total bacterial dark DIC uptake (TB_{DIC}), total bacterial dark DIC uptake contribution (TB_{DIC} %), primary production (PP), particulate organic carbon (POC), temperature (Temp), bacterial production (BP), nitrate (NO_3), chlorophyll-*a* concentration (Chl-*a*), and bacterial abundance. * $p < 0.01$. ** $p < 0.001$. *** $p < 0.0001$.

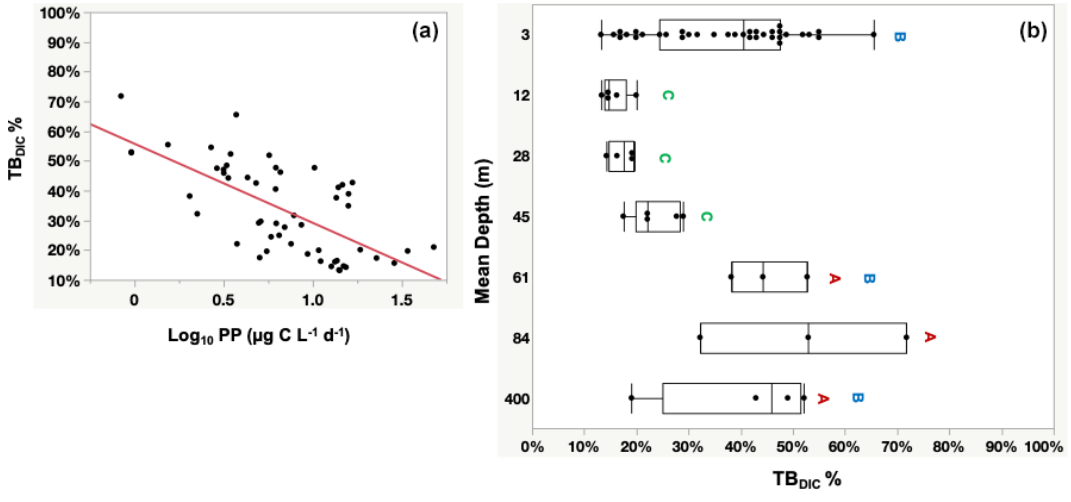

Figure 5. Panel **(a)** shows the significant probability of the relationship between the percentage contribution of TB_{DIC} (TB_{DIC} %) and the primary productivity (PP), whereas **(b)** shows the total bacterial DIC uptake contribution (TB_{DIC} %) to the total DIC fixation within the photic zone and the deep 400 m. The boxes with the same letters are not statistically significant, as determined by pairwise comparisons via Student's *t* test. Each box plot indicates the 95 % confidence intervals with ± 1 SD. The central line in the box represents the median for each group of samples.

to those reported from oligotrophic ocean waters (Alonso-Sáez et al., 2010; Llirós et al., 2011; Zhou et al., 2017). The deepest dark CO_2 fixation rate measurement reported so far was carried out in the Mediterranean Sea at 4900 m, estimated at $0.096 \pm 0.02\,\mu g\,C\,L^{-1}\,d^{-1}$ (Yakimov et al., 2014). We recorded a relatively high TB_{DIC} uptake rate in Red Sea surface waters, toward the base of the photic zone but reaching high values at 400 m. Increases in dark DIC fixation rates have been observed in the tropical South China Sea at depths between 200 and 1500 m, with rates even exceeding those at the surface (Zhou et al., 2017). The high TB_{DIC} values reported in the surface and deep water in our study suggest that dark DIC fixation contributes significantly not only to the carbon fixation dynamics of surface water, where bacterial abundance is high, but also throughout the entire (oxygenated) water column (Reinthaler et al., 2010; Yakimov et al., 2014; Zhou et al., 2017). Therefore, given the high TB_{DIC} values measured in the oligotrophic Red Sea ecosystem, our findings highlight the importance of accounting for dark DIC fixation in total carbon production estimations.

The Red Sea is characterized by a warm temperature throughout the water column (Shaltout, 2019), with an average temperature of 21.46 ± 0.23 °C at 400 m depth recorded in our study. Here, temperature was found to have a positive correlation with PP but no correlation with the TB_{DIC} uptake rate, whereas Chl *a* had no correlation with PP as PP decreased gradually down the photic zone, while Chl *a* showed the maximum values at the bottom of the photic zone. However, Chl *a* showed a positive correlation with TB_{DIC}. Nitrate showed a negative correlation with PP, suggesting nitrate depletion by the more productive phytoplankton communities, whereas TB_{DIC} was positively correlated with PP. Studies conducted in the North Atlantic Ocean and tropical estuarine systems have reported a weak relationship between dark CO_2 fixation and temperature, nutrients, and Chl *a* (Reinthaler et al., 2010; Signori et al., 2018). In contrast, a study conducted in the South China Sea reported that dark CO_2 fixation rates increased in with temperature and nutrient concentration (Zhou et al., 2017).

TB_{DIC} % contribution was calculated from the TB_{DIC} uptake rate relative to the sum of the independent PP measured in the light and the independent TB_{DIC} measured in the dark. The significantly negative relationship between the TB_{DIC} % contribution and PP confirmed the relevance of the dark CO_2 fixation to the most oligotrophic waters. The bacterial dark CO_2 fixation rate (TB_{DIC}) contributed significantly to the total DIC uptake within the photic zone, where it reached up to 72 % of the photosynthetic primary production and up to 52 % of the surface PP in the deep water at 400 m. In the eastern North Atlantic Ocean, the dark CO_2 fixation was reported to support 72 % of the prokaryotic carbon demand in the mesopelagic layers below 200 m (Baltar et al., 2010). Baltar and Herndl (2019) analyzed data collected over the course of 30 years and found that the dark CO_2 uptake rate contributed up to 22 % of the total PP in the euphotic layer (0–150 m). Additionally, increasing evidence has suggested that dark CO_2 uptake by heterotrophic bacteria contributes significantly to surface CO_2 fixation, contributing up to 30 % of the DIC uptake in some oligotrophic waters (González et al., 2008; Palovaara et al., 2014). Similarly, in our study we recorded an average contribution of TB_{DIC} to total DIC uptake of 33.95 % within the photic zone and the deep 400 m water. The increase in the contribution of TB_{DIC} to the carbon flux with decreasing PP in the Red Sea highlights the importance of dark DIC fixation as a key mechanism driving plankton communities, particularly in highly oligotrophic environments with low (surface) or absent (deep water) primary production. Additionally, the relevance of dark CO_2 incorporation is likely significant in oligotrophic and nutrient-depleted environments where the availability of labile organic carbon is limited (González et al., 2008; Alonso-Sáez et al., 2010). Overall, our results confirm the relevance of dark CO_2 fixation to the oligotrophic Red Sea.

Our findings indicate that TB_{DIC} exceeded HBP, as reported in previous studies (Zhou et al., 2017), confirming the important role of TB_{DIC} in fueling bacterial metabolism in oligotrophic waters, with low levels of labile organic matter for bacterial growth such as surface and deep oligotrophic waters. Although in our study we refer to bacterial production, archaea can contribute to BP and in a higher proportion to the dark DIC uptake than bacteria. A study conducted in the northern Red Sea (Gulf of Aqaba) indicated that 10 %–15 % of leucine incorporation could be attributed to archaeal activity or to bacteria unaffected by the added antibiotics (Ionescu et al., 2009). However, they found that the impact of adding antibiotics to the incubations largely inhibited dark CO_2 incorporation, although it was minor below the photic layer, suggesting that a large proportion of the dark DIC uptake was due to archaea in the deep waters (Ionescu et al., 2009). In addition, they found that the impact of antibiotics largely inhibited dark CO_2 incorporation, indicating that most of the dark DIC uptake was due to bacteria (Ionescu et al., 2009).

The high TB_{DIC} contribution to total DIC uptake observed in our study can support the growth of the bacterial community, providing a path to support bacterial metabolism, respiration, and carbon flux in the microbial loop (Zhou et al., 2017). The importance of dark CO_2 fixation processes seemed to increase with depth in the Red Sea, as the dark / light ratio of CO_2 fixation rate increased in deeper waters, reaching up to 1.13 ± 0.65 toward the base of the photic zone. These findings were consistent with those of Baltar and Herndl (2019), who reported that the dark / light ratio reached 1 at 120–160 m depths from data collected along the ALOHA and BATS datasets, the longest oceanic time series of the Atlantic and Pacific oceans, highlighting the urgent need to account for dark DIC fixation in future studies on total primary production. Considering the total net primary production in the ocean to be approximately $50\,Pg\,C\,yr^{-1}$ as reported by Field et al. (1998) and based on the potential

TB_{DIC} % contribution of 13.18 % to 71.78 % to the $total_{DIC}$ fixation reported in our study, we estimated that approximately 6.5 to as much as 35.5 Pg C yr^{-1} could be added to the global primary production estimation. This would be a considerable amount of carbon productivity by heterotrophic microbes that is not being accounted for in current carbon flux and production estimations, which could represent a significant source of carbon in surface and deep waters (Baltar and Handle, 2019).

5 Conclusions

Using a stable-isotope method, our study demonstrated the substantial contribution of dark CO_2 assimilation by heterotrophic bacteria in the oligotrophic Red Sea. The results presented herein represent a first attempt to estimate and confirm the role of dark heterotrophic bacteria CO_2 assimilation to the carbon flux dynamics along the Red Sea at different depths and in different water bodies. Even though temperature, a uniquely influential feature of the warm Red Sea, appeared to have a weak correlation with TB_{DIC}, our study confirmed that the importance of anaplerotic CO_2 incorporation and chemoautotrophic process would be significant in environments with low or absent primary productivity. Moreover, due to the large fraction of $total_{DIC}$ fixation generated from the contribution of TB_{DIC} in the surface and the deep water, as reported in our study and other studies, it is essential to account for the contribution of heterotrophic dark CO_2 fixation to the total DIC fixation as a source of prokaryotic carbon demand.

Data availability. The data are presented in the article (Tables 1 and 2) and can be requested from the corresponding author.

Author contributions. Each of the authors made substantial contributions to the conception, design, and execution of this study. SA was responsible for the development of the study design and goals, data analyses, critical revisions of the manuscript, and overall project coordination. CMD contributed to the development of the study design, interpretation of the data, and critical revisions of the manuscript, in addition to his coordination in conducting the project. In addition, CMD provided the raw data run by a Picarro CRDS in his laboratory. DLS was involved in the data collection and analyses and provided critical feedback on the manuscript. AA was responsible for data collection, data analyses, and drafting the manuscript. In addition, AA reviewed any critical revisions made by the co-authors. All authors have read and approved the final manuscript for submission.

Competing interests. The contact author has declared that none of the authors has any competing interests.

Disclaimer. Publisher's note: Copernicus Publications remains neutral with regard to jurisdictional claims in published maps and institutional affiliations.

Acknowledgements. We would like to express our deepest gratitude to each and every person involved in this study and the King Abdullah University of Science and Technology, who made this research possible. First and foremost, we would like to express our gratitude to and thank all participants who generously shared their time and experiences enclosed in this research, including all crew members and scientific leaders of the vessels and cruises involved in this study. In addition, we would like to thank the Coastal & Marine Resources Core Lab (CMR) team at the King Abdullah University of Science and Technology (KAUST), who were behind the possibility of conducting the outdoor setup of the coastal experiments. We also extend our appreciation to Mongi Ennasri, who provided the support and assistance throughout the samples analyses in the Picarro CRDS. The support of each and every one of these individuals and organizations enabled us to collect and analyze the data and to disseminate our findings. We would like to express our appreciation and gratitude to the associate editor and the reviewers for their contributions to the improvement of this paper. Their expertise, meticulous attention to detail, and thoughtful feedback have played a crucial role in refining and strengthening the content of this work. We are sincerely grateful for their time, dedication, and commitment to advancing scholarly knowledge in this field.

Financial support. This work was supported by the King Abdullah University of Science and Technology (KAUST).

Review statement. This paper was edited by Steven Bouillon and reviewed by Federico Baltar and Marc Llirós Dupré.

References

Alonso-Sáez, L., Galand, P. E., Casamayor, E. O., Pedros-Alio, C., and Bertilsson, S.: High bicarbonate assimilation in the dark by Arctic bacteria, ISME J., 4, 1581–1590, 2010.

Azam, F., Fenchel, T., J. G., Gray, J. S., Meyer-Reil, L. A., and Thingstad, F.: The ecological role of water-column microbes in the sea, Mar. Ecol.-Prog. Ser., 10, 257–263, 1983.

Baltar, F. and Herndl, G. J.: Ideas and perspectives: Is dark carbon fixation relevant for oceanic primary production estimates?, Biogeosciences, 16, 3793–3799, https://doi.org/10.5194/bg-16-3793-2019, 2019.

Baltar, F., Arístegui, J., Sintes, E., Gasol, J. M., Reinthaler, T., and Herndl, G. J.: Significance of non-sinking particulate organic carbon and dark CO_2 fixation to heterotrophic carbon demand in the mesopelagic northeast Atlantic, Geophys. Res. Lett., 37, L09602, https://doi.org/10.1029/2010GL043105, 2010.

Baltar, F., Lundin, D., Palovaara, J., Lekunberri, I., Reinthaler, T., Herndl, G. J., and Pinhassi, J.: Prokaryotic responses to ammonium and organic carbon reveal alternative CO_2 fixation pathways and importance of alkaline phosphatase in

the mesopelagic North Atlantic, Front. Microbiol., 7, 1670, https://doi.org/10.3389/fmicb.2016.01670, 2016.

Berden, G., Peeters, R., and Meijer, G.: Cavity ring-down spectroscopy: Experimental schemes and applications, Int. Rev. Phys. Chem., 19, 565–607, 2000.

Braun, A., Spona-Friedl, M., Avramov, M., Elsner, M., Baltar, F., Reinthaler, T., Herndl, G. J., and Griebler, C.: Reviews and syntheses: Heterotrophic fixation of inorganic carbon – significant but invisible flux in environmental carbon cycling, Biogeosciences, 18, 3689–3700, https://doi.org/10.5194/bg-18-3689-2021, 2021.

Boschker, H. T. S. and Middelburg, J. J.: Stable isotopes and biomarkers in microbial ecology, FEMS Microbiol. Ecol., 40, 85–95, 2002.

Chaidez, V., Dreano, D., Agusti, S., Duarte, C. M., and Hoteit, I.: Decadal trends in Red Sea maximum surface temperature, Sci. Rep., 7, 1–8, 2017.

Dickson, A. G., Sabine, C. L., and Christian, J. R.: Guide to best practices for ocean CO_2 measurements, North Pacific Marine Science Organization, PICES Special Publication 3; IOCCP Report 8, 191, https://doi.org/10.25607/OBP-1342, 2007.

Dijkhuizen, L. and Harder, W.: Current views on the regulation of autotrophic carbon dioxide fixation via the Calvin cycle in bacteria, Antonie van Leeuwenhoek, 50, 473–487, 1984.

Ducklow, H. and Kirchman, D.: Bacterial production and biomass in the oceans, Microbial Ecology of the Oceans, 1, 85–120, 2000.

Edwards, F. J.: Climate and oceanography, Red sea, 1, 45–68, 1987.

Erb, T. J.: Carboxylases in natural and synthetic microbial pathways, Appl. Environ. Microb., 77, 8466–8477, 2011.

Field, C. B., Behrenfeld, M. J., Randerson, J. T., and Falkowski, P.: Primary production of the biosphere: integrating terrestrial and oceanic components, Science, 281, 237–240, 1998.

Gasol, J. M. and Morán, X. A. G.: Flow cytometric determination of microbial abundances and its use to obtain indices of community structure and relative activity, in: Hydrocarbon and Lipid Microbiology Protocols, edited by: McGenity, T. J., Timmis, K. N., and Nogales, B., Springer, Berlin, Heidelberg, 159–187, 2016.

González, J. M., Fernández-Gómez, B., Fernàndez-Guerra, A., Gómez-Consarnau, L., Sánchez, O., Coll-Lladó, M., Del Campo, J., Escudero, L., Rodríguez-Martínez, R., Alonso-Sáez, L., and Latasa, M.: Genome analysis of the proteorhodopsin-containing marine bacterium Polaribacter sp. MED152 (Flavobacteria), P. Natl. Acad. Sci. USA, 105, 8724–8729, 2008.

Grasshoff, K.: Zur Chemie des Roten Meeres und des Inneren Golfs von Aden : nach beobachtungen von F. S. "Meteor" während der Indischen Ozean Expedition 1964/65, Meteor Forschungsergebnisse: Reihe A, Allgemeines, Physik und Chemie des Meeres, 6, 1–76, 1969.

Hansen, H. P. and Koroleff, F.: Determination of Nutrients, Methods of Seawater Analysis, edited by: Grasshoff, K., Kremling, K., and Ehrhardt, M., 159–228, https://doi.org/10.1002/9783527613984.ch10, 1999.

Ionescu, D., Penno, S., Haimovich, M., Rihtman, B., Goodwin, A., Schwartz, D., Hazanov, L., Chernihovsky, M., Post, A. F., and Oren, A.: Archaea in the Gulf of Aqaba, FEMS Nicrobiol. Ecol., 69, 425–438, 2009.

Kirchman, D. L.: Uptake and regeneration of inorganic nutrients by marine heterotrophic bacteria, Microbial Ecology of the Oceans, 28, 255–271, 2000.

Koshikawa, H., Harada, S., Watanabe, M., Kogure, K., Ioriya, T., Kohata, K., Kimura, T., Sato, K., and Akehata, T.: Influence of plankton community structure on the contribution of bacterial production to metazooplankton in a coastal mesocosm, Mar. Ecol.-Prog. Ser., 186, 31–42, https://doi.org/10.3354/meps186031, 1999.

Li, W. K. W. and Dickie, P. M.: Light and dark ^{14}C uptake in dimly-lit oligotrophic waters: relation to bacterial activity, J Plankton Res., 13, 29–44, 1991.

Li, W. K. W., Irwin, B. D., and Dickie, P. M.: Dark fixation of ^{14}C: variations related to biomass and productivity of phytoplankton and bacteria, Limnol. Oceanogr., 38, 483–494, 1993.

Llirós, M., Alonso-Sáez, L., Gich, F., Plasencia, A., Auguet, O., Casamayor, E. O., and Borrego, C. M.: Active bacteria and archaea cells fixing bicarbonate in the dark along the water column of a stratified eutrophic lagoon, FEMS Microbiol. Ecol., 77, 370–384, 2011.

López-Sandoval, D. C., Delgado-Huertas, A., and Agustí, S.: The ^{13}C method as a robust alternative to ^{14}C-based measurements of primary productivity in the Mediterranean Sea, J. Plankton Res., 40, 544–554, 2018.

López-Sandoval, D. C., Delgado-Huertas, A., Carrillo-de-Albornoz, P., Duarte, C. M., and Agustí, S.: Use of cavity ring-down spectrometry to quantify ^{13}C-primary productivity in oligotrophic waters, Limnol. Oceanogr.-Meth., 17, 137–144, 2019.

López-Sandoval, D. C., Duarte, C. M., and Agustí, S.: Nutrient and temperature constraints on primary production and net phytoplankton growth in a tropical ecosystem, Limnol. Oceanogr., 66, 2923–2935, 2021.

Markager, S.: Dark uptake of inorganic ^{14}C in oligotrophic oceanic waters, J. Plankton Res., 20, 1813–1836, 1998.

Middelburg, J. J., Barranguet, C., Boschker, H. T., Herman, P. M., Moens, T., and Heip, C. H.: The fate of intertidal microphytobenthos carbon: An in situ ^{13}C-labeling study, Limnol. Oceanogr., 45, 1224–1234, 2000

Nielsen, E. S.: Dark fixation of CO_2 and measurements of organic productivity. With remarks on chemo-synthesis, Physiol. Plantarum, 13, 348–357, 1960.

Palovaara, J., Akram, N., Baltar, F., Bunse, C., Forsberg, J., Pedrós-Alió, C., González, J. M., and Pinhassi, J.: Stimulation of growth by proteorhodopsin phototrophy involves regulation of central metabolic pathways in marine planktonic bacteria, P. Natl. Acad. Sci. USA, 111, E3650–E3658, 2014.

Prabowo, D. A. and Agusti, S.: Free-living dinoflagellates of the central Red Sea, Saudi Arabia: Variability, new records and potentially harmful species, Mar. Pollut. Bull., 141, 629–648, 2019.

Prakash, A., Sheldon, R. W., and Sutcliffe Jr., W. H.: Geographic variation of oceanic ^{14}C dark uptake, Limnol. Oceanogr., 36, 30–39, 1991.

Reinthaler, T., van Aken, H. M., and Herndl, G. J.: Major contribution of autotrophy to microbial carbon cycling in the deep North Atlantic's interior, Deep-Sea Res. Pt. II, 57, 1572–1580, 2010.

Roslev, P., Larsen, M. B., Jørgensen, D., and Hesselsoe, M.: Use of heterotrophic CO_2 assimilation as a measure of metabolic activity in planktonic and sessile bacteria, J. Microbiol. Meth., 59, 381–393, 2004.

Shaltout, M.: Recent Sea surface temperature trends and future scenarios for the Red Sea, Oceanologia, 61, 484–504, 2019.

Signori, C. N., Valentin, J. L., Pollery, R. C., and Enrich-Prast, A.: Temporal variability of dark carbon fixation and bacterial production and their relation with environmental factors in a tropical estuarine system, Estuar. Coast., 41, 1089–1101, 2018.

Steemann-Nielsen, E.: On the determination of the activity for measuring primary production, J. Cons. Int. Explor. Mer., 18, 117–140, 1952.

Wafar, M., Qurban, M. A., Ashraf, M., Manikandan, K. P., Flandez, A. V., and Balala, A. C.: Patterns of distribution of inorganic nutrients in Red Sea and their implications to primary production, J. Marine Syst., 156, 86–98, 2016.

Wood, H. G. and Werkman, C. H.: The utilisation of CO_2 in the dissimilation of glycerol by the propionic acid bacteria, Biochem. J., 30, 48–53, https://doi.org/10.1042/bj0300048, 1936.

Yakimov, M. M., La Cono, V., Smedile, F., Crisafi, F., Arcadi, E., Leonardi, M., Decembrini, F., Catalfamo, M., Bargiela, R., Ferrer, M., and Golyshin, P. N.: Heterotrophic bicarbonate assimilation is the main process of de novo organic carbon synthesis in hadal zone of the Hellenic Trench, the deepest part of Mediterranean Sea, Env. Microbiol. Rep., 6, 709–722, 2014.

Yao, F. and Hoteit, I.: Rapid red sea deep water renewals caused by volcanic eruptions and the North Atlantic oscillation, Sci. Adv., 4, eaar5637, https://doi.org/10.1126/sciadv.aar5637, 2018.

Zhou, W., Liao, J., Guo, Y., Yuan, X., Huang, H., Yuan, T., and Liu, S.: High dark carbon fixation in the tropical South China Sea, Cont. Shelf Res., 146, 82–88, 2017.